Published in final edited form as:

Hepatology. 2016 May ; 63(5): 1576–1591. doi:10.1002/hep.28468.

A new HIF-1α/RANTES driven pathway to hepatocellular carcinoma mediated by germline haploinsufficiency of SART1/HAF

Mei Yee Koh[1], **Mihai Gagea**[2], **Timothy Sargis**[1], **Robert Lemos Jr**[1], **Geoffrey Grandjean**[1], **Adriana Charbono**[1], **Vasileos Bekiaris**[1], **John Sedy**[1], **Galina Kiriakova**[2], **Xiuping Liu**[2], **Lewis R. Roberts**[3], **Carl Ware**[1], and **Garth Powis**[1]

[1]Sanford Burnham Prebys Medical Discovery Institute, La Jolla, CA

[2]The University of Texas M.D. Anderson Cancer Center, Houston, TX

[3]Mayo Clinic, Rochester MN

Abstract

The hypoxia inducible factor, HIF-1 is a central regulator of the response to low oxygen or inflammatory stress and plays an essential role in the survival and function of immune cells. However, the mechanisms regulating non-hypoxic induction of HIF-1 remain unclear. Here, we assess the impact of germline heterozygosity of a novel, oxygen independent ubiquitin ligase for HIF-1α; the hypoxia associated factor, HAF (encoded by *SART1*). *SART1*$^{-/-}$ mice were embryonic lethal, whereas male *SART1*$^{+/-}$ mice spontaneously recapitulated key features of non-alcoholic steatohepatitis (NASH) driven HCC including steatosis, fibrosis and inflammatory cytokine production. Male but not female *SART1*$^{+/-}$ mice showed significant upregulation of HIF-1α in circulating and liver-infiltrating immune cells but not in hepatocytes prior to the development of malignancy. Additionally, Kupffer cells derived from male but not female *SART1*$^{+/-}$ mice produced increased levels of the HIF-1 dependent chemokine, RANTES, compared to wild-type. This was associated with increased liver-neutrophilic infiltration whereas infiltration of lymphocytes and macrophages were not significantly different. Neutralization of circulating RANTES decreased liver neutrophilic infiltration, and attenuated HCC tumor initiation/growth in *SART1*$^{+/-}$ mice. *Conclusion*: We establish a new tumor suppressor role for HAF in immune cell function by preventing inappropriate HIF-1 activation in male mice, and identify RANTES as a novel therapeutic target for NASH and NASH-driven HCC.

Keywords

Hypoxia; neutrophils; CCL5; NAFLD NASH

Hypoxia is a state of reduced oxygen pressure below its physiological threshold, which impacts both normal and disease processes (1, 2). Hypoxia characterizes virtually every site

Corresponding author: (mkoh@sbpdiscovery.org).

No conflict of interest is declared.

of inflammation, thus requiring infiltrating immune cells to undergo a metabolic switch towards anerobic pathways to maintain energy requirements. The hypoxia inducible factor (HIF) transcription factors are central regulators of the hypoxic response. The HIFs are heterodimers comprising one of three major oxygen labile HIF-α subunits (HIF-1α, HIF-2α and HIF-3α), and a constitutive HIF-1β subunit, which together form the HIF-1, HIF-2 and HIF-3 transcriptional complexes respectively (3). HIF-1 plays an essential role in the survival and function of immune cells, by facilitating energy generation through anerobic glycolysis (4). Under aerobic conditions, HIF-α is hydroxylated by oxygen-dependent prolyl-hydroxylases, promoting ubiquitination by the von Hippel-Lindau protein (pVHL) E3 ligase complex resulting in HIF-α proteasomal degradation (5). Under hypoxic conditions, pVHL binding is abrogated, HIF-α is stabilized and heterodimerizes with HIF-1β to transactivate a variety of hypoxia-responsive genes (6). HIF-1α can also be induced under non-hypoxic conditions by pro-inflammatory cytokines, which allow the initiation of an inflammatory response before tissues become hypoxic (4, 7). In addition to pVHL, the hypoxia associated factor, HAF (encoded by *SART1*), is an isoform specific E3 ubiquitin ligase that specifically degrades HIF-1α (but not HIF-2α), in an oxygen-independent manner (8). Also known as SART1, HAF is expressed in both normal and malignant proliferating tissue (9, 10), is important for spliceosome assembly (11), and cell division (12). Here, we address the physiological role of HAF.

Experimental Procedures

Generation of mice

The *SART1*$^{+/-}$ mice were derived from the Texas Institute for Genomic Medicine gene trap C57BL/6 SART1$^{-/-}$ ES cell line (Clone IST11321E11). Genotyping was performed using allele-specific PCR (Supplemental methods). All animal procedures were performed in accordance with institutional animal care and use protocols.

Gene expression analyses

Differential gene expression profiling of *SART1*$^{+/-}$ versus wild-type livers (3 replicates each) were performed using the GeneChip® Mouse Genome 430 2.0 Array and the 3′ IVT PLUS Reagent Kit (Affymetrix, P/N 902416, Santa Clara CA); GEO Accession GSE71057. Data analysis was performed using Transcriptome Analysis Console 2.0, which generated the heatmaps, and Ingenuity Pathway Analysis (Qiagen Inc., Valencia CA). Hit validation was performed by Taqman custom arrays (Life Technologies, Carlsbad CA).

Human liver sections

Human HCC (of unknown etiology, Fig 8A**)** was purchased from US Biomax Inc (Rockville, MD). Sections in Fig 8B-D were from formalin fixed paraffin-embedded non-alcoholic steatohepatitis (NASH) associated HCC tumors collected during surgical resections and liver transplants (normal liver samples) at the Mayo Clinic between 1997 and 2013. Sections were examined by pathologist, graded histologically and classified by etiology. The study was approved by the Mayo Clinic Institutional Review Board.

MRI and RANTES study

MRI was performed by operators blinded to study design using a Bruker 11.7T MRI system (Supplemental methods). After initial imaging, tumor-bearing mice were stratified into 2 groups and injected IP with 400μg RANTES neutralizing antibody (MAB478, R&D systems, Minneapolis MN) or saline twice per week for 5 weeks, after which mice were re-imaged and tumor volumes were recalculated.

Statistical analyses

These were performed using Student's T-tests using Graphpad Prism 6 or Microsoft Excel. $p<0.05$ were considered significant with $*p < 0.05$, $**p < 0.01$.

All other methods are listed in Supplemental methods.

Results

SART1 deficiency is embryonic lethal at E11.5

HAF heterozygous mice ($SART1^{+/-}$) were generated using C57BL/6 embryonic stem cells produced by the gene trap method (Fig. 1A-B). Tissue-wide profiling of male wild-type and $SART1^{+/-}$ mice confirmed expression of HAF in multiple organs including skin, lung, heart, liver, kidney, spleen and colon, with highest expression within the spleen (Fig. 1C). HAF heterozygosity was associated with significant decreases of HAF in heart, liver and kidney, and caused more subtle decreases in other tissues in which HAF could be detected (Fig. 1C-D).

Out of a total of 99 pups resulting from pairings with heterozygous parents, 70 were het, whereas 29 were wild-type, close to the expected ratio of 2:1:1 for het: wild-type: knockout, consistent with embryonic lethality. By genotyping embryos at various developmental stages, knockouts were only identified at E11.5, and $SART1^{-/-}$ embryos showed diminished size and vascularization compared to their heterozygous or wild-type littermates (Fig. 1E). Thus, knockout of *SART1* results in embryonic lethality at approximately E11.5.

SART1 haploinsufficiency promotes hepatic steatosis and HCC—Despite the embryonic lethality ofHAF knockout mice, mice heterozygous for HAF ($SART1^{+/-}$) appeared to develop normally, and displayed no anatomically observable defects. However, at >14 months, male $SART1^{+/}$ mice were significantly smaller, and had ruffled fur compared to their wild-type counterparts (Fig. 2A and Supplemental Data S1A). Necropsy revealed multifocal large liver tumors (histologically confirmed as HCC) in ~83% (5/6) of male $SART1^{+/-}$ mice, which were absent from their wild-type littermates (Fig. 2A), whereas both wild-type and $SART1^{+/-}$ male mice exhibited severe hepatic steatosis. The livers of the $SART1^{+/-}$ mice displayed hallmarks of non-alcoholic steatohepatitis (NASH)-driven HCC including hepatic steatosis (confirmed by Oil Red O staining), fibrosis (confirmed by Sirius Red staining) and foci of immune cell infiltration (Fig. 2B, Fig.4E-F). Visual analysis of additional male $SART1^{+/-}$ mice confirmed grossly visible tumors in an additional 90% (9/10) of mice. By contrast, the livers of age-matched $SART1^{+/-}$ females showed minimal steatosis, and no malignant tumors were detected either grossly or histologically (0/4, not

shown). At age 10 months, HCC was detected in 42% (5/12) of mice, whereas pre-neoplastic foci of hepatocellular alterations and/or adenomas were present in 83% (10/12) of mice. By contrast, none were observed in wild-type littermates (Fig. 2A). Consistent with enlarged livers and decreased overall body weight, the average liver weights/body weight ratios in *SART1*$^{+/-}$ mice were also significantly higher than their wild-type counterparts (Fig. 2C, **RHS**). Liver tumors were detected by MRI in a further 57% (4/7) of male *SART1*$^{+/-}$ mice aged 16-18 months (S1B), but were not detected in male mice under the 10 months (0/21), nor in female *SART1*$^{+/-}$ mice aged 16-19 months (0/3). The rapid growth of the liver tumors was apparent when we monitored tumor growth in one 1616-18 month old mouse, where we found multiple large liver tumor nodules (S1C) confirmed histologically as HCC. No other obvious abnormalities were observed in the blood or any of the other major organs apart from age-related changes. Hence, germline haploinsufficiency of HAF promotes spontaneous HCC development only in male mice > age 10 months.

Hepatic steatosis precedes HCC formation in livers of *SART1*$^{+/-}$ mice

When examined histologically, livers of 1-month-old *SART1*$^{+/-}$ mice were indistinguishable from those of their wild-type littermates (Fig. 2D**).** However, at age 6 months, *SART1*$^{+/-}$ liverslivers showed moderate to marked microvesicular hepatic steatosis with increased severity in the centrilobular/periacinar and midzonal regions, and also showed multiple foci of altered hepatocytes with atypical nuclei (Fig. 2E, 3A). These foci were composed of hypertrophic or cytomegalic hepatocytes and showed increased proliferation supported by the increased number of mitotic and binucleated hepatocytes. Although these foci are considered pre-neoplastic lesions predisposing to tumor development, no neoplastic lesions were observed at this age. By contrast, livers of wild-type littermates showed only very mild steatosis, and no pre-neoplastic lesions. Consistent with the age-related progression to HCC, the elevation of the serum transaminases alanine aminotransferase (ALT), aspartate aminotransferase (AST), or alkaline phosphatase (ALP) in the *SART1* $^{+/-}$ mice versus wild type become apparent from 6 months of age (S1D). The age-associated liver phenotypes of the *SART1*$^{+/-}$ mice are summarized in Fig. 3B and S1E. Intriguingly, although HAF levels in *SART1*$^{+/-}$ versus wild-type livers were not significantly different at age 1 month, HAF levels decreased with increasing age, which reflected the development of liver pathology in the *SART1* $^{+/-}$ mice (Fig. 3C-D). Hence, although initially normal, the livers of *SART1*$^{+/-}$ mice first manifest foci of pre-neoplastic hepatocellular alteration, coinciding with the development of hepatic steatosis, which then progress to HCC.

Microarray analysis of SART1$^{+/-}$ mouse livers indicate metabolic and immune dysfunction—To evaluate global changes in gene expression associated with HCC in the *SART1* $^{+/-}$ mice, we performed microarray analysis comparing a *SART1* $^{+/-}$liver tumor (T) to an age-matched wild-type liver (N). Using a fold change cut-off of 2.0 fold up-or-down regulated, and $p<0.05$, 2290 genes were differentially expressed in T vs N groups out of 20185 total genes probed by the array (Fig. 3E). Intriguingly, the top differentially expressed gene was alpha fetoprotein (*Afp*, 441 fold induction versus normal), which encodes a blood serum marker typically used for diagnosis of HCC in humans (S2A). Using Ingenuity Pathway Analysis (IPA), the top biological functions associated with these differentially expressed genes were those involved in the inflammatory response, cancer, and lipid

metabolism (S2B). We also observed highly significant changes in genes associated with hepatocyte hyperplasia/proliferation, steatosis and HCC. All these expression changes were consistent with the observed steatosis/steatohepatitis/HCC phenotype in the *SART1*$^{+/-}$ livers.

SART1 $^{+/-}$ hepatocytes have defective fatty acid oxidation—To investigate the molecular pathogenesis of hepatic steatosis in the *SART1*$^{+/-}$ mice, we examined the expression of subsets of genes known to be involved in the various aspects of lipid metabolism. According to IPA, 39 out of 45 genes involved in fatty acid metabolism were significantly decreased (p=6.86E-13; Fig. 3E, S3A). This included Acyl-CoA synthase long-chain family member 1 (*Acsl1*), which catalyzes one of the first steps of fatty acid oxidation; and a large number of cytochrome P450 (CYP) genes, which have diverse roles in liver metabolism (13). By contrast, levels of the major transcription factors that promote lipogenesis and lipid uptake, sterol regulatory element–binding protein-1c (SREBP-1c, *SREBF1),* carbohydrate response element binding protein (ChREBP, *MLXIPL*), and peroxisome proliferator-activated receptor gamma (PPAR-γ, *PPARG*), were not significantly altered in our dataset, nor were their downstream gene expression profiles significantly altered. The trend of decreased expression of genes involved in fatty acid oxidation was validated using 3 additional *SART1*$^{+/-}$ livers normalized to livers from 3 wild-type littermates, and was also confirmed at the protein level for Acsl1 and CYP2b10 (Fig. 3F).

To determine whether fatty acid oxidation was indeed dysfunctional in the *SART1*$^{+/-}$ mice, hepatocytes from 4 month old *SART1*$^{+/-}$ mice and their wild-type littermates were subjected to metabolic analysis using the Seahorse XF Extracellular Flux analyzer. Using oxygen consumption rate, OCR, as an indicator of mitochondrial respiration, we found that *SART1*$^{+/-}$ hepatocytes showed a lower basal level of respiration compared to wild-type (Fig. 4A). When treated with the mitochondrial uncoupler FCCP, which induces maximal respiration, *SART1*$^{+/-}$ hepatocytes showed an almost 4-fold decrease in the ability to utilize exogenous palmitate compared to wild-type hepatocytes (Fig. 4A-B). Similar results were obtained using Huh7 human hepatoma cells transiently transfected with control or HAF (*SART1*) siRNA (Fig. 4C-D). Thus, the enhanced hepatic steatosis observed in the *SART1* $^{+/-}$ livers is likely due to defective fatty acid oxidation. .

SART1$^{+/-}$ mice show marked upregulation of HIF-1α in immune cells—In addition to metabolic dysfunction, *SART1* $^{+/-}$ livers showed changes consistent with increased inflammatory cell activation and trafficking (Fig. 3E, S2B). Indeed, *SART1*$^{+/-}$ livers showed extensive immune cell infiltration, distributed randomly and sporadically, often in clusters, throughout the liver parenchyma (Fig. 4E). These included cells positive for F4/80 or Ly6G suggesting that these clusters contained macrophages and neutrophils respectively (Fig. 4F). Additionally, Kupffer cell hyperplasia (likely a result of phagocytosis of disrupted hepatocytes) was observed in 100% (6/6) of the *SART1*$^{+/-}$ livers but not in wild-type livers (S1E). Significantly, the liver-infiltrating immune cells were markedly HIF-1α positive in *SART1*$^{+/-}$ but not in wild-type livers (arrows, Fig. 4G). Increases in HIF-1α was manifest primarily in *SART1*$^{+/-}$ immune cells, but not in *SART1*$^{+/-}$ hepatocytes, suggesting that the HIF-1α upregulation was not due to a general hypoxic

environment within the livers (Fig. 4G, S4A-B). The changes observed in *SART1*$^{+/-}$ immune cells may also reflect the distribution of HAF expression, which was detected primarily in infiltrating immune cells in wild-type livers (S4C). By contrast, HIF-2α was expressed in the immune infiltrating cells in the livers of both wild-type and *SART1*$^{+/-}$ mice (S4C*).*

To establish whether HIF-1α upregulation played a causal role in HCC carcinogenesis in the *SART*$^{+/-}$ mice, or occurred as a result of the HCC already present, we isolated mononuclear cells from peripheral blood (PBMCs) and spleens of 6 month old *SART1*$^{+/-}$ and wild-type mice. HIF-1α protein levels were significantly elevated in both PBMCs and splenocytes from *SART1*$^{+/-}$ versus wild type mice, but not in primary hepatocytes (Fig. 5A, S4B). We also noted that unlike the PBMCs, splenocytes did not express detectable HIF-1α unless exposed to hypoxia (only cells exposed to hypoxia are depicted), suggesting some intrinsic differences in HIF-1α expression in these cell types. These findings were associated with a reduction in HAF protein levels expected of the *SART1*$^{+/-}$ genotype (S4D). By contrast, we did not detect upregulation of HIF-1α in PBMCs or splenocytes isolated from 6 month old female *SART1*$^{+/-}$ mice, and only detected subtle decreases in HAF levels (S5A-B). Hence, the data suggest that HIF-1α upregulation in immune cells was intrinsic to the male *SART1*$^{+/-}$ mice, and occurred independently of HCC.

To determine whether HAF expression in immune cells was cell type-specific, we measured the activity of the LacZ reporter transgene used to disrupt the *SART1* gene. We detected LacZ positivity in a wide variety of cell populations including spleen- and bone marrow-derived cells, and peripheral blood leukocytes (Fig 5B, S6A). To identify cell types that expressed LacZ (and therefore endogenous HAF), we stained splenocytes with surface markers: CD19 (B-Cells), TCRβ (T-Cells), Ly6G (neutrophils), F4/80 (macrophages) prior to the Lac Z activity assay. Here, we observed significant LacZ/FITC positivity in all cell types, with highest expression in B and T-cells, and macrophages, whereas no significant differences between the immune cell populations from *SART1*$^{+/-}$ and wild-type mice were observed (Fig. 5C, S6B-C). Thus, HAF is highly expressed in all immune cells, and loss of HAF in the male *SART1*$^{+/-}$ mice is associated with HIF-1α upregulation in all immune cell types.

HCC is preceded by increased RANTES secretion and elevated neutrophilic infiltration—To determine whether immune cells played a causal role in the development of HCC, we isolated Kupffer cells (KCs) from the livers of 5-month-old *SART1*$^{+/-}$ mice, and compared their secreted cytokine expression profiles to that of wild-type littermates. In general, *SART1*$^{+/-}$ KCs had higher levels of secreted cytokines than wild-type KCs (Fig. 5D, S3B). Intriguingly, levels of the chemokine Regulated on Activation, Normal T cell Expressed (RANTES) was increased by >100 fold in the *SART1*$^{+/-}$ KCs compared to wild-type KCs (Fig. 5D). RANTES plays a major role in recruiting leukocytes to sites of injury, and is transcriptionally regulated by HIF-1α by multiple functional HREs within its promoter (14, 15). Knockdown of HAF using siRNA in THP-1 cells also resulted in significant upregulation of RANTES in both normoxia and hypoxia (Fig. 5E). *RANTES* was significantly upregulated in the livers of *SART1*$^{+/-}$ mice over wild-type mice from 6 months of age, although increased transcription was already detected at 1 month of age (Fig. 6A).

Consistent with HIF-1α upregulation, we also detected an age-dependent albeit delayed increase (compared to RANTES) in the transcription of HIF-1 target genes facilitated glucose transporter 1 (*Slc2a1*), Hexokinase 1 (*Hk1*) and pyruvate kinase (muscle) 1 (*Pkm1*) in the $SART1^{+/-}$ livers indicating a general shift towards glycolytic metabolism (Fig. 6B). By contrast, we did not observe any differences in secretion of RANTES or other cytokines by KCs from similar-aged female $SART1^{+/-}$ livers compared to wild-type (S5C).

To determine whether the immune cell sub-populations present within the $SART1^{+/-}$ livers were altered prior to HCC initiation, we profiled the livers of 66 month old mice. Intriguingly, we found a 6-fold increase in Ly6G+ neutrophils in $SART1^{+/-}$ livers relative to wild-type, also observed via immunohistochemistry, whereas levels of CD11c+ macrophages, CD4, CD8, gamma delta and NK T cells were not significantly altered (Fig. 6C-D). We also observed a 3-fold increase in Ly6G+ neutrophils within livers of 1 month old $SART1^{+/-}$ mice which was not observed in the spleens, suggesting that increased neutrophilic infiltration was an early event independent of hepatic steatosis, and was not due to systemic elevation of the neutrophil population (Fig. 6E-F, S7). Thus, male but not female $SART1^{+/-}$ KCs secrete elevated levels of cytokines/chemokines including a >100-fold increase in RANTES. This was associated with increased neutrophilic infiltration in male $SART1^{+/-}$ livers prior to the development of steatosis or HCC.

RANTES neutralization inhibits HCC initiation/growth and decreases neutrophil infiltration—To determine the impact of RANTES secretion on liver neutrophilic infiltration, and HCC initiation/progression, we used a neutralizing antibody to RANTES and monitored treatment efficacy by MRI. Imaging of $SART1^{+/-}$ mice aged 14-18 months revealed only 4 of 15 mice bore tumors with a total volume of >100mm^3 clearly detectable by MRI (Fig. 7A, S8). The mice were treated with RANTES neutralizing antibody (or saline) for 5 weeks and were re-imaged. Upon re-imaging, we observed the appearance of new nodules in the control group but not in the RANTES-treated group, suggesting that RANTES treatment prevented liver tumor initiation/promotion (Fig. 7A-C, S8). The growth of individual nodules was also markedly reduced in the RANTES-treated mice (RANTES 6.709 ± 3.872 fold, n=5, versus control 13.20 ± 6.546 fold, n=5; Fig. 7D-E). We also observed a significant decrease in Ly6G+ infiltrating neutrophils in both tumor and adjacent normal tissue of mice treated with RANTES compared to those treated with saline alone (Fig. 7F-G). Hence RANTES neutralization inhibits both the initiation/promotion and growth of liver tumors, and attenuates neutrophilic infiltration in the livers of $SART1^{+/-}$ mice.

Human HCC show upregulation of HIF-1α/RANTES and HAF downregulation—Similar to the $SART1^{+/-}$ livers (Fig. 4G), HIF-1α positive immune infiltrating cells in the context of largely HIF-1α negative hepatocytes was also observed in human HCC including NASH-derived HCC (Fig. 8A-B). RANTES expression in both hepatocytes and immune infiltrating cells was also upregulated in NASH-derived HCC compared to normal liver (Fig. 8C). By contrast, HAF staining was detected primarily in infiltrating cells in normal human liver but was largely negative in human NASH-derived HCC (Fig. 8A, D), thus supporting a role for HAF as a tumor suppressor for HCC.

Discussion

HCC is the most common primary malignancy of the liver, with more than 750,000 new patients diagnosed globally each year (16). HCC frequently develops in the context of chronic hepatitis, which may arise from infection with Hepatitis B virus (HBV) or Hepatitis C virus (HCV), and from alcoholic or non-alcoholic fatty liver disease (AFLD/NAFLD) (17). The current obesity epidemic has been associated with an increasing prevalence of NAFLD and its inflammatory component non-alcoholic steatohepatitis (NASH), which leads to HCC. The complex interplay between damaged hepatocytes and immune infiltrating cells within an inflammatory hepatic microenvironment is believed to drive HCC initiation and progression (18, 19). Hence, HCC pathogenesis has been described by the “two hit” hypothesis whereby the first “hit”-steatosis/viral infection - sensitizes the liver to a variety of second “hits”, such as oxidative stress and abnormal cytokine production, which lead to necroinflammation and fibrosis (20, 21).

Here, we show that germline haploinsufficiency of *SART1* induces HCC in the context of NASH only in male mice. This is to our knowledge, the only genetic model where haploinsufficency promotes HCC without requiring any further manipulation. The livers of the $SART1^{+/-}$ mice showed decreased fatty acid oxidation, providing a likely mechanism for the hepatic steatosis (or first ‘hit’), and also showed constitutive stabilization of HIF-1α specifically in immune cells, elevated cytokine secretion by KCs, and increased neutrophilic infiltration prior to HCC development (together constituting the second ‘hit’). The activation of these immune cells likely promotes oxidative damage and inflammation, driving progression to HCC. Although infiltrating immune cells are known to be involved in HCC initiation and progression, the plethora of inflammatory cytokines upregulated in human HCC have confounded the identification of individual key cytokines to target for therapy (22-25). The robust timeline for HCC development in the male $SART1^{+/-}$ mice enabled the identification of RANTES as an early, non-redundant event driving HCC initiation and progression, likely by promoting neutrophil infiltration. Intriguingly, increased circulating RANTES has been associated with obesity in humans, and is upregulated in patients with NAFLD/NASH, suggesting that RANTES might be involved in the progression to NASH-driven HCC (26, 27). The evaluation of the relevance of HIF-1/RANTES to NASH-driven HCC is currently being investigated in a larger patient set. Intriguingly, RANTES elevation has also been observed in patients with alcoholic and viral hepatitis, whereas RANTES polymorphisms correlate to susceptibility to HCC suggesting that RANTES may be a valid therapeutic target for HCC regardless of etiology (28, 29).

An intriguing observation in our studies was that HCC did not occur in female $SART1^{+/-}$ mice. This male predominance also occurs in human HCC, and in chemically-induced HCC in mice (with the hepatic procarcinogen N-nitrosodiethylamine, DEN) (30, 31). The male bias for DEN-induced HCC has been attributed to the suppressive effect of estrogen on IL-6 production, aa driving factor for DEN-induced HCC (30). Whether the male bias observed in our model is related to IL-6 production is unclear, but it does appear to be associated with an intrinsic resistance of both wild-type and $SART1^{+/-}$ female mice to hepatic steatosis, an initiating factor for HCC in the male $SART1^{+/-}$ mice. Female $SART1^{+/-}$ and wild-type mice even at >16 months of age develop only mild hepatic steatosis, if at all, and do not become

obese like their male counterparts (our unpublished observations). The age-dependent decrease in HAF levels in male *SART1*$^{+/-}$ mice, which was accompanied by immune cell specific upregulation of HIF-1α, was not observed in female mice suggesting that the predisposition to steatosis in males may drive further decreases in HAF, hence exacerbating the development of liver pathology (Fig 3C, 5A, S5). Additional factors driving the male bias may be the sex-dependent production of RANTES (Fig 5D, S5C), which has been previously reported in obese mice (26). Nevertheless, steatosis per se is insufficient to induce HCC as germline *VHL*$^{+/-}$ mice, or mice bearing hepatocyte-specific VHL deletion, develop severe hepatic steatosis but not HCC (32, 33). Since VHL is unable to degrade HIF-1α under hypoxic conditions, it is possible that HAF, as an oxygen-independent ubiquitin ligase, may play a more central role in attenuating inappropriate HIF-1α upregulation under hypoxic, inflammatory conditions. Indeed, the high expression levels of endogenous HAF within the mouse spleen and in immune infiltrating cells (Fig. 1C, 8A, D) supports an immune-specific physiological role of HAF as a suppressor of HIF-1α.

In view of the systemic activation of immune mediators in male *SART1*$^{+/-}$ mice, we also observed increased lymphohistiocytic infiltration in the lungs, gastro-intestinal tract, and lymph nodes of *SART1*$^{+/-}$ mice compared to wild-type (our unpublished observations). Hence, it is likely that other organ-specific stresses may lead to inflammation-induced cancer in these organs, and this is currently under investigation. In addition to its role as a ubiquitin ligase for HIF-1α, HAF has also been known to play a role in pre-mRNA splicing (11), and to inhibit Hepatitis C virus (HCV) replication in hepatoma cells via changes in splicing (34). Hence, splicing changes in the *SART1*$^{+/-}$ mouse are also currently being explored.

In conclusion, this study identifies a novel tumor suppressor function of HAF by maintaining regular hepatic metabolism, and in preventing inappropriate immune cell activation, possibly by suppressing HIF-1α. Additionally, we described a novel mouse model of NASH-derived HCC, which closely recapitulates the human disease. Our findings highlight a central role of the HIF-1/RANTES axis in HCC initiation and progression, thus identifying a novel target for therapy.

Supplementary Material

Refer to Web version on PubMed Central for supplementary material.

Acknowledgements

The authors would like to thank Catherine D. Moser and Nasra H. Giama from Mayo Clinic for liver tissue preparation and curation.

Financial support: R01CA181106 (MYK), R01CA098920 (GP), R01CA164679 and P01CA177322 (CW), P30DK084567 and Mayo Clinic Cancer Center grant CA15083 (LRR) , and the SBP NCI Cancer Center Support Grant P30 CA030199. The content is solely the responsibility of the authors and does not necessarily represent the official views of the National Institutes of Health.

References

1. Imtiyaz HZ, Simon MC. Hypoxia-inducible factors as essential regulators of inflammation. Current topics in microbiology and immunology. 2010; 345:105–120. [PubMed: 20517715]
2. Koh MY, Powis G. Passing the baton: the HIF switch. Trends Biochem Sci. 2012; 37:364–372. [PubMed: 22818162]
3. Wang GL, Jiang BH, Rue EA, Semenza GL. Hypoxia-inducible factor 1 is a basic-helix-loop-helix-PAS heterodimer regulated by cellular O2 tension. Proc Natl Acad Sci U S A. 1995; 92:5510–5514. [PubMed: 7539918]
4. Cramer T, Yamanishi Y, Clausen BE, Förster I, Pawlinski R, Mackman N, Haase VH, et al. HIF-1α Is Essential for Myeloid Cell-Mediated Inflammation. Cell. 2003; 112:645–657. [PubMed: 12628185]
5. Jaakkola P, Mole DR, Tian YM, Wilson MI, Gielbert J, Gaskell SJ, Kriegsheim A, et al. Targeting of HIF-alpha to the von Hippel-Lindau ubiquitylation complex by O2-regulated prolyl hydroxylation. Science. 2001; 292:468–472. [PubMed: 11292861]
6. Maxwell PH, Pugh CW, Ratcliffe PJ. Activation of the HIF pathway in cancer. Curr Opin Genet Dev. 2001; 11:293–299. [PubMed: 11377966]
7. Zinkernagel A, Johnson R, Nizet V. Hypoxia inducible factor (HIF) function in innate immunity and infection. Journal of Molecular Medicine. 2007; 85:1339–1346. [PubMed: 18030436]
8. Koh MY, Darnay BG, Powis G. Hypoxia-associated factor, a novel E3-ubiquitin ligase, binds and ubiquitinates hypoxia-inducible factor 1alpha, leading to its oxygen-independent degradation. Mol Cell Biol. 2008; 28:7081–7095. [PubMed: 18838541]
9. Shichijo S, Nakao M, Imai Y, Takasu H, Kawamoto M, Niiya F, Yang D, et al. A gene encoding antigenic peptides of human squamous cell carcinoma recognized by cytotoxic T lymphocytes. J Exp Med. 1998; 187:277–288. [PubMed: 9449708]
10. Sasatomi T, Yamana H, Shichijo S, Tanaka S, Okamura T, Ogata Y, Itoh K, et al. Expression of the SART1 tumor-rejection antigens in colorectal cancers. Dis Colon Rectum. 2000; 43:1754–1758. [PubMed: 11156463]
11. Makarova OV, Makarov EM, Luhrmann R. The 65 and 110 kDa SR-related proteins of the U4/U6.U5 tri-snRNP are essential for the assembly of mature spliceosomes. EMBO J. 2001; 20:2553–2563. [PubMed: 11350945]
12. Kittler R, Putz G, Pelletier L, Poser I, Heninger AK, Drechsel D, Fischer S, et al. An endoribonuclease-prepared siRNA screen in human cells identifies genes essential for cell division. Nature. 2004; 432:1036–1040. [PubMed: 15616564]
13. Schoonjans K, Staels B, Grimaldi P, Auwerx J. Acyl-CoA synthetase mRNA expression is controlled by fibric-acid derivatives, feeding and liver proliferation. European Journal of Biochemistry. 1993; 216:615–622. [PubMed: 8375397]
14. Karlmark KR, Wasmuth HE, Trautwein C, Tacke F. Chemokine-directed immune cell infiltration in acute and chronic liver disease. Expert Rev Gastroenterol Hepatol. 2008; 2:233–242. [PubMed: 19072358]
15. Yeligar SM, Machida K, Tsukamoto H, Kalra VK. Ethanol Augments RANTES/CCL5 Expression in Rat Liver Sinusoidal Endothelial Cells and Human Endothelial Cells via Activation of NF-κB, HIF-1α, and AP-1(). Journal of immunology (Baltimore, Md. : 1950). 2009; 183:5964–5976.
16. Ferlay J, Shin H-R, Bray F, Forman D, Mathers C, Parkin DM. Estimates of worldwide burden of cancer in 2008: GLOBOCAN 2008. International Journal of Cancer. 2010; 127:2893–2917. [PubMed: 21351269]
17. El-Serag HB. Hepatocellular Carcinoma. New England Journal of Medicine. 2011; 365:1118–1127. [PubMed: 21992124]
18. Grivennikov SI, Greten FR, Karin M. Immunity, Inflammation, and Cancer. Cell. 2010; 140:883–899. [PubMed: 20303878]
19. Scarzello AJ, Jiang QJ, Back T, Dang H, Hodge D, Hanson C, Subleski J, et al. LTβR signalling preferentially accelerates oncogenic AKT-initiated liver tumours. Gut. 2015 In press.
20. Day CP, James OFW. Steatohepatitis: A tale of two “hits”? Gastroenterology. 1998; 114:842–845. [PubMed: 9547102]

21. Browning JD, Horton JD. Molecular mediators of hepatic steatosis and liver injury. The Journal of Clinical Investigation. 2004; 114:147–152. [PubMed: 15254578]
22. Schall TJ, Bacon K, Toy KJ, Goeddel DV. Selective attraction of monocytes and T lymphocytes of the memory phenotype by cytokine RANTES. Nature. 1990; 347:669–671. [PubMed: 1699135]
23. Xu R, Huang H, Zhang Z, Wang F-S. The role of neutrophils in the development of liver diseases. Cell Mol Immunol. 2014; 11:224–231. [PubMed: 24633014]
24. Liu C, Tao Q, Sun M, Wu JZ, Yang W, Jian P, Peng J, et al. Kupffer cells are associated with apoptosis, inflammation and fibrotic effects in hepatic fibrosis in rats. Lab Invest. 2010; 90:1805–1816. [PubMed: 20921949]
25. Wilson CL, Jurk D, Fullard N, Banks P, Page A, Luli S, Elsharkawy AM, et al. NF[kappa]B1 is a suppressor of neutrophil-driven hepatocellular carcinoma. Nat Commun. 2015; 6
26. Wu H, Ghosh S, Perrard XD, Feng L, Garcia GE, Perrard JL, Sweeney JF, et al. T-Cell Accumulation and Regulated on Activation, Normal T Cell Expressed and Secreted Upregulation in Adipose Tissue in Obesity. Circulation. 2007; 115:1029–1038. [PubMed: 17296858]
27. Kirovski G, Gäbele E, Dorn C, Moleda L, Niessen C, Weiss TS, Wobser H, et al. Hepatic steatosis causes induction of the chemokine RANTES in the absence of significant hepatic inflammation. International Journal of Clinical and Experimental Pathology. 2010; 3:675–680. [PubMed: 20830238]
28. Maltby J, Wright S, Bird G, Sheron N. Chemokine levels in human liver homogenates: associations between GRO alpha and histopathological evidence of alcoholic hepatitis. Hepatology. 1996; 24:1156–1160. [PubMed: 8903391]
29. Tsai H-T, Yang S-F, Chen D-R, Chan S-E. CCL5-28, CCL5-403, and CCR5 genetic polymorphisms and their synergic effect with alcohol and tobacco consumptions increase susceptibility to hepatocellular carcinoma. Medical Oncology. 2012; 29:2771–2779. [PubMed: 22374185]
30. Naugler WE, Sakurai T, Kim S, Maeda S, Kim K, Elsharkawy AM, Karin M. Gender Disparity in Liver Cancer Due to Sex Differences in MyD88-Dependent IL-6 Production. Science. 2007; 317:121–124. [PubMed: 17615358]
31. Park EJ, Lee JH, Yu G-Y, He G, Ali SR, Holzer RG, Österreicher CH, et al. Dietary and Genetic Obesity Promote Liver Inflammation and Tumorigenesis by Enhancing IL-6 and TNF Expression. Cell. 2010; 140:197–208. [PubMed: 20141834]
32. Rankin EB, Higgins DF, Walisser JA, Johnson RS, Bradfield CA, Haase VH. Inactivation of the Arylhydrocarbon Receptor Nuclear Translocator (Arnt) Suppresses von Hippel-Lindau Disease-Associated Vascular Tumors in Mice. Molecular and Cellular Biology. 2005; 25:3163–3172. [PubMed: 15798202]
33. Haase VH, Glickman JN, Socolovsky M, Jaenisch R. Vascular tumors in livers with targeted inactivation of the von Hippel–Lindau tumor suppressor. Proceedings of the National Academy of Sciences. 2001; 98:1583–1588.
34. Lin W, Zhu C, Hong J, Zhao L, Jilg N, Fusco DN, Schaefer EA, et al. The spliceosome factor SART1 exerts its anti-HCV action through mRNA splicing. Journal of Hepatology. 2015; 62:1024–1032. [PubMed: 25481564]

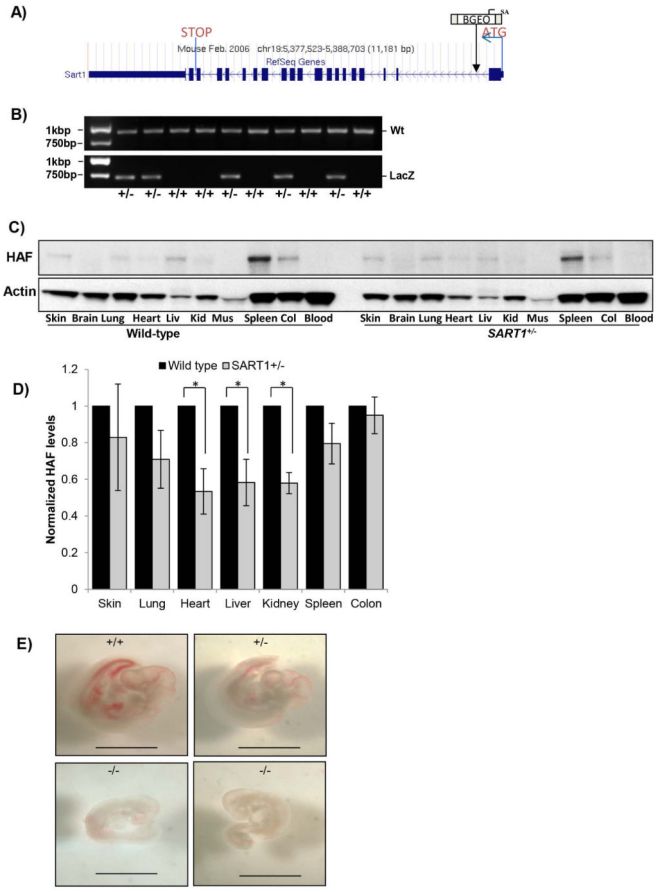

Figure 1. Generation *SART1* knockout and heterozygous mice

A) Gene trap construct used to disrupt the HAF (*SART1)* gene. B) Genotyping of *SART1* mice. C) HAF levels in a panel of tissues from 2-month old male $SART1^{+/-}$ and wild-type mice with quantitation in (D) (4mice/group, 20μg protein/lane). Data are the mean ± SE. E) Images of $SART1^{+/+}$, $SART1^{+/-}$, and $SART1^{-/-}$ embryos at E11.5. Scale bar = 200μM.

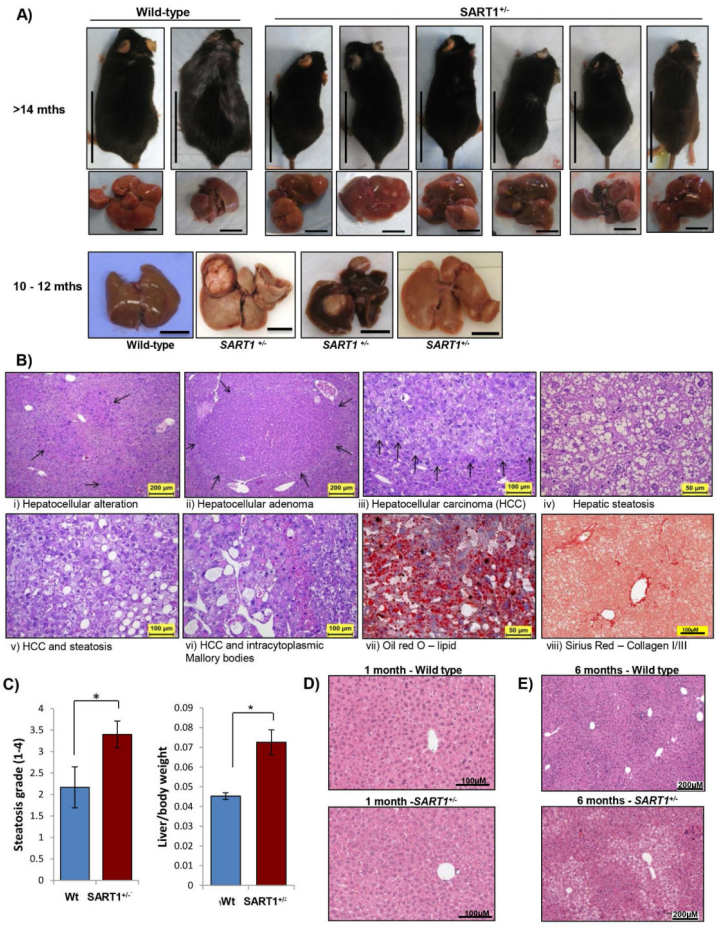

Figure 2. Liver pathology in male *SART1*$^{+/-}$ mice

A) Male *SART1*$^{+/-}$ and wild-type mice with associated livers at age >14 months; and 10-12 months. Scale bar: 5cm (mice); 1cm (livers). B) Hematoxylin and eosin (H&E) stained sections showing indicated pathological changes of *SART1*$^{+/-}$ livers. C) Liver steatosis grade and liver/body weight ratios of wild type (n=6) and *SART1*$^{+/-}$ (n=12) mice of age 10-12 months (mean ± SE). D-E) H&E sections of wild-type and *SART1*$^{+/-}$ livers at age 1 month (D) and 6 months (E).

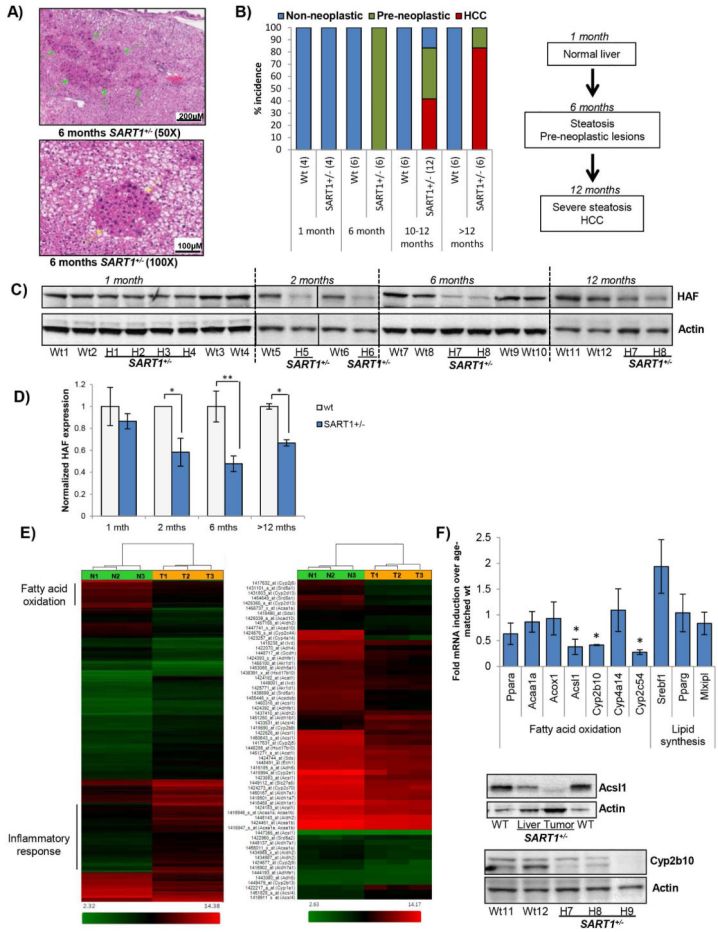

Figure 3. Hepatic steatosis precedes HCC in male *SART1*$^{+/-}$ mice

A) H&E sections showing microvesicular hepatic steatosis and pre-neoplastic foci of cellular alteration in 6 month old *SART1*$^{+/-}$ livers. B) Quantitation and flowchart of age-related progression of liver pathology in male *SART1*$^{+/-}$ mice versus wild-type littermates. [#mice]. C) Western blot showing HAF expression in wild-type and *SART1*$^{+/-}$ livers according to age with quantitation (D). E) Gene expression heatmap of a *SART1*$^{+/-}$ liver tumor (T) normalized to a wild type liver (N) showing regions enriched for genes involved in fatty acid oxidation (FAO), and the inflammatory response with enlarged heatmap showing FAO genes at RHS. F) Taqman validation for a select number of FAO genes using 3 additional mice/group with western blot validation.

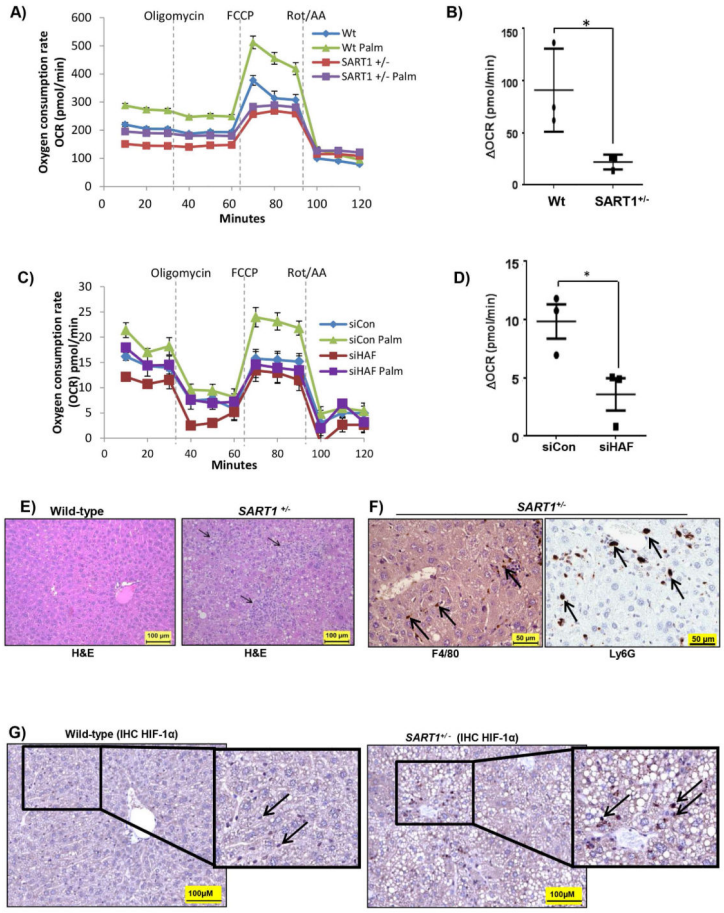

Figure 4. *SART1*$^{+/-}$ livers manifest metabolic dysfunction and increased inflammatory activation

Representative experiments showing Seahorse metabolic analysis of oxygen consumption rate (OCR) of, A) primary hepatocytes isolated from male *SART1*$^{+/-}$ or wild-type mice (aged 4 months) with quantitation of data (3 mice/group) shown in B; or C) Huh7 cells transfected with HAF siRNA with quantitation of data from 3 replicate wells shown in (D). Data are mean ± SD. E-G) IHC of liver sections using; E) H&E : showing infiltration of inflammatory cells; F) F4/80 and Ly6G: indicating infiltration of macrophages and neutrophils respectively (arrows); and G) HIF-1α; in *SART1*$^{+/-}$ and wild-type livers (aged 12 months).

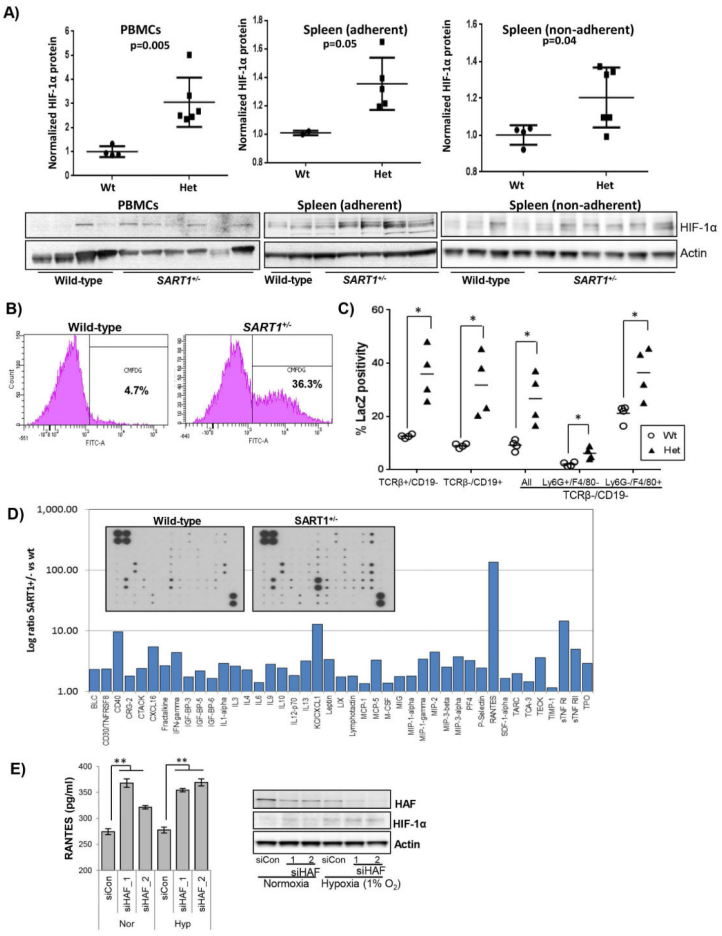

Figure 5. HAF loss is associated with increased HIF-1α and RANTES production

A) Western blot and quantitation of HIF-1α levels in peripheral blood mononuclear cells (PBMCs), spleen adherent and spleen non-adherent mononuclear cells from male *SART1*$^{+/-}$ and wild-type mice (aged 6 months). B) Flow cytometry scatterplots showing LacZ-FITC intensity in peripheral blood cells from male *SART1*$^{+/-}$ and wild-type mice (aged 4 months). C) Lac Z intensities of immune cells from the spleens of male *SART1*$^{+/-}$ (Het) and wild-type (Wt) mice (aged 4 months, 4 mice/group). Each data point represents a single mouse with mean ± SD. D) Quantitation secreted cytokines from Kupffer cells (KCs) isolated from male *SART1*$^{+/-}$ livers normalized to wild-type with arrays depicted inset (pooled from 4 mice/group). E) Quantitation of RANTES secretion by THP-1 cells transfected with siRNAs to HAF with western blot validation on RHS. Data are mean ± SE.

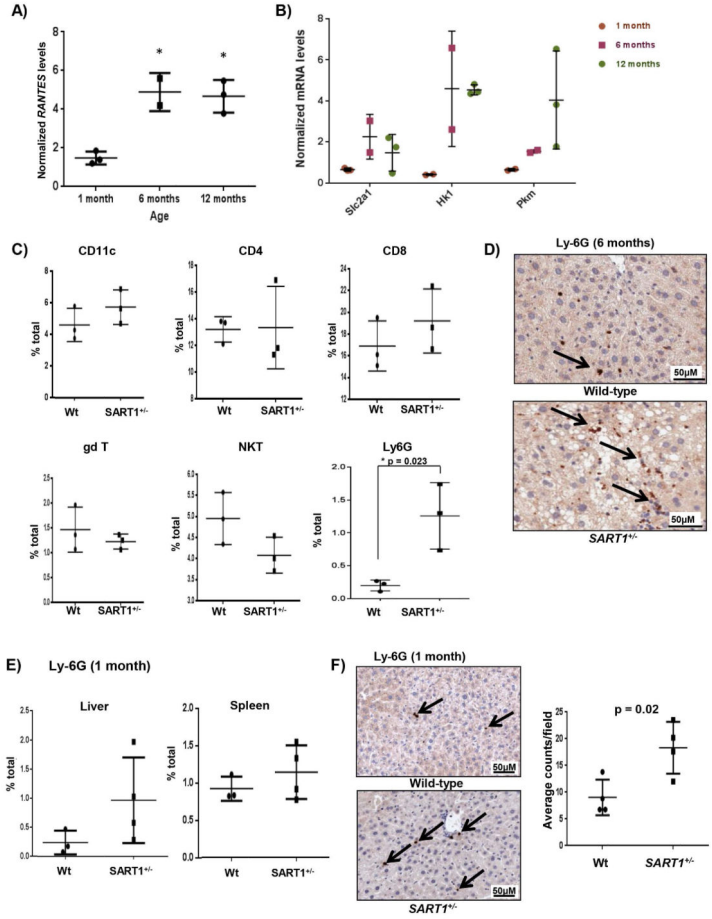

Figure 6. RANTES upregulation is associated with increased liver neutrophilic infiltration

Age-related transcription of A) *RANTES,* and B) HIF-1 dependent glycolytic genes, *SLCA1, HK1*, and *PKM* in *SART1*$^{+/-}$ livers normalized to wild-type determined by qRT-PCR. C) Quantitation of immune cell populations within the livers of 6 month old male *SART1*$^{+/-}$ and wild-type mice using indicated markers (3 mice per group). D) IHC for Ly6G + cells (neutrophils) in *SART1*$^{+/-}$ and wild-type livers (6 months old). E) Quantitation of Ly6G+ cells within livers and spleens of 1 month old mice determined by flow cytometry. F) IHC for Ly6G+ cells in livers of 1-month-old mice with quantitation showed on RHS. Each data point represents a single mouse with mean ± SD.

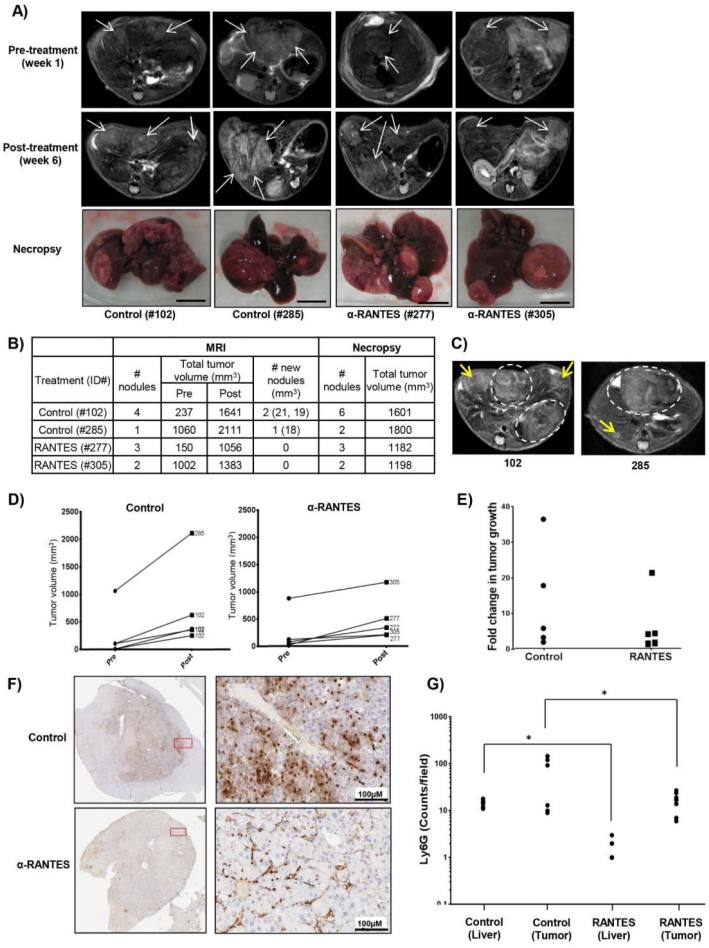

Treatment (ID#)	MRI				Necropsy	
	# nodules	Total tumor volume (mm³)		# new nodules (mm³)	# nodules	Total tumor volume (mm³)
		Pre	Post			
Control (#102)	4	237	1641	2 (21, 19)	6	1601
Control (#285)	1	1060	2111	1 (18)	2	1800
RANTES (#277)	3	150	1056	0	3	1182
RANTES (#305)	2	1002	1383	0	2	1198

Figure 7. Neutralization of RANTES attenuates liver neutrophilic infiltration and inhibits HCC initiation and progression

A) Pre-and post-treatment axial MRI liver slices of male *SART1*$^{+/-}$ mice aged 16-18 months, and images of livers upon necropsy. Arrows indicate tumor nodules. Scale bar = 1 cm. B) Quantitation of tumor volume and number detected by MRIs in comparison to actual values determined by necropsy. C) Post-treatment MRIs of indicated mice with new tumor nodules (yellow arrows) and previously detected nodules (dotted ovals). Growth rate (D), or fold change (E) of individual tumor nodules in control and RANTES-treated mice. F) IHC for Ly6G in tumors from control and RANTES-treated mice with quantitation in (G) (4 random fields/tissue type/mouse).

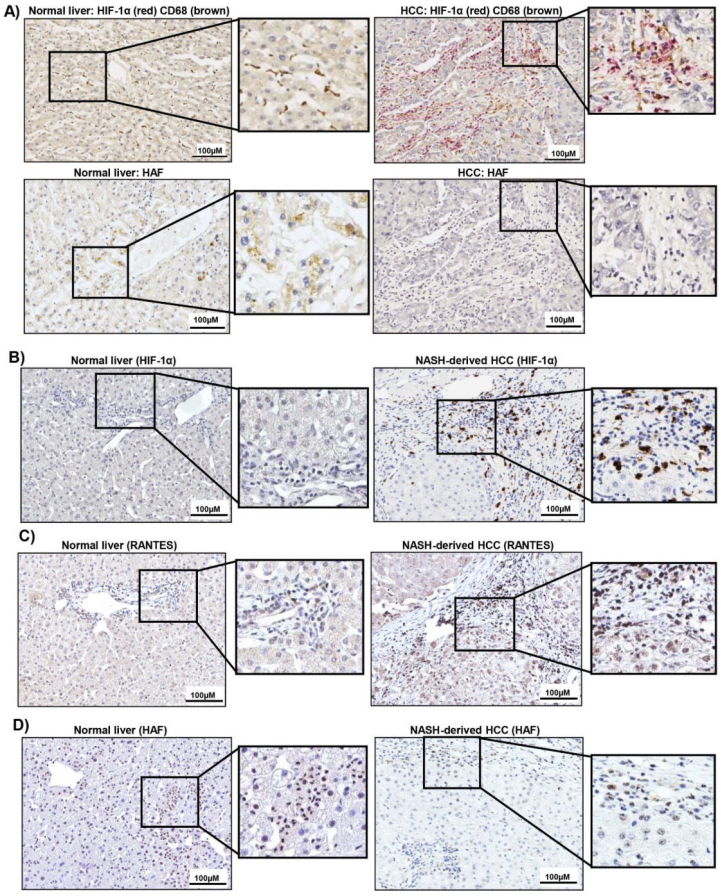

Figure 8. Levels of HIF-1α, HAF and RANTES in human HCC

A) Dual IHC for HIF-1α (red) and CD68 (brown) or HAF (below) in normal liver and human HCC of unknown etiology. B-D) IHC for HIF-1α (B), RANTES (C),) and HAF (D) in normal liver or NASH-derived HCC. Enlarged regions are indicated.